PHYSICAL REVIEW D VOLUME 25, NUMBER 3 1 FEBRUARY 1982

Neutrino counting through pair production by muons

V. Barger
Physics Department, University of Wisconsin, Madison, Wisconsin 53706

W. Y. Keung
Brookhaven National Laboratory, Upton, New York 11973

R. J. N. Phillips
Rutherford and Appleton Laboratories, Chilton, Didcot, Oxon, England
(Received 8 September 1981)

We calculate the cross section and scattered-muon distributions for the process $\mu+Z\to\mu+\nu+\bar{\nu}+Z$, namely neutrino pair production by muons in the Coulomb field of a heavy nucleus. The cross section is a measure of the number of light-neutrino flavors, assuming the standard model, as previously recognized. The differential distributions of the scattered muon are needed to interpret any partial measurement (short of a total cross section) and also provide important consistency checks for an eventual experimental signal. Unfortunately, the predicted cross section is very small for a small number of flavors; also, the final muon energy peaks near zero so that the practical acceptance is reduced. A measurement of this cross section is therefore not foreseen in the near future, despite its interest. We also calculate the contribution expected from diffractive vector-meson production $\mu+Z\to\mu+V^0+Z$ with $V^0\to\nu\bar{\nu}$ decay; the $V^0=\psi$ contribution considerably exceeds the direct neutrino rate. However, the V^0 process yields a completely different muon spectrum and can be distinguished by this; it also offers an independent measure of the number of neutrino flavors.

I. INTRODUCTION

Lepton pair production by leptons in a Coulomb field has long been studied as a possible way to investigate weak interactions in purely leptonic sectors.[1] Recently, it has been recognized that for the particular case of neutrino pair production by muons,

$$\mu+Z\to\mu+\nu+\bar{\nu}+Z\ , \tag{1}$$

the cross section in the standard electroweak model depends directly on the number of light-neutrino flavors and therefore offers a way to measure the latter.[2] In principle, there is a clean experimental signature—one scattered muon with no visible hadronic energy and large missing energy—so that measurements may eventually be feasible.[3] It is already known that the cross section is very small, but previous calculations either omit the neutral-current contributions[1] or contain errors of sign in some terms.[2] In the present paper we give a new and simple cross-section formula and calculate the numerical predictions for coherent production from Fe and H nuclei, including dependence on incident muon polarization. To elucidate eventual measurements, we also present the scattered-muon distributions and discuss the contributions of diffractive neutral-vector-meson production $\mu N\to\mu V^0 N$ with $V^0\to\nu\bar{\nu}$ decay ($V^0=\rho^0,\omega,\psi,\cdots$).

Regrettably, the neutrino-pair-production cross section is extremely small at presently accessible energies, for a small number of neutrino flavors. Also, the final-muon spectrum peaks near zero, so that with typical muon acceptance cuts, many of the events would be lost. A measurement of this cross section therefore seems unlikely in the near future. However, it appears that the V^0 production background would not be a serious problem and should be viewed instead as an asset; although the cross section from ψ is much bigger than direct neutrino pair production, it leads to a characteristically different muon spectrum and can be discriminated on this basis. Since it too depends on the number of neutrino flavors, it offers an independent measure of this number.

Other backgrounds can be imagined, such as charged-current interactions $\mu N\to\nu X$, $\bar{\mu}N\to\bar{\nu}X$,

where the recoiling final system X includes a decay muon plus little other visible energy. These contributions can be inferred from a detailed analysis of the crossed reactions $\nu N \to \mu X$, $\bar{\nu} N \to \bar{\mu} X$ in the quark-parton framework; alternatively, since they are simply the tails of continua, they can be extracted directly from experiment by extrapolating the hadronic energy distribution.

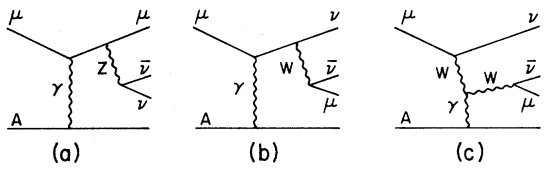

FIG. 1. Feynman diagrams for neutrino pair production by muons.

II. CROSS-SECTION FORMULAS

The reaction of Eq. (1) proceeds by the Feynman diagrams of Fig. 1 (where the crossed bremsstrahlung diagrams are omitted for brevity). Figure 1(a) shows the process of principal interest, which produces neutrino pairs of all flavors and gives the dependence on flavor number. Figure 1(b) contributes only $\nu_\mu \bar{\nu}_\mu$ pairs. Figure 1(c) is required by gauge invariance, but in the usual gauges it is negligible at present energies because it has an extra heavy boson propagator. The reaction $\mu Z \to \tau \bar{\nu}_\tau \nu_\mu Z \to \mu \nu_\mu \bar{\nu}_\mu \nu_\tau \bar{\nu}_\tau Z$, analogous to Fig. 1(b) with $\tau \to \mu \nu \bar{\nu}$ decay, has a similar experimental signature, but a much smaller cross section, which we neglect also.

The relevant four-lepton couplings appearing in Figs. 1(a) and 1(b) can be written in terms of the following two effective Hamiltonians[2,4]:

$$\mathscr{H}^Z = \frac{G_F}{\sqrt{2}} \bar{\psi}_\mu \gamma^\alpha (g_V - g_A \gamma_5) \psi_\mu \left[\sum_i \bar{\psi}_{\nu_i} \gamma_\alpha (1-\gamma_5) \psi_{\nu_i} \right] , \tag{2}$$

$$\mathscr{H}^W \frac{G_F}{\sqrt{2}} \bar{\psi}_\mu \gamma^\alpha (1-\gamma_5) \psi_\mu \bar{\psi}_{\nu_\mu} \gamma_\alpha (1-\gamma_5) \psi_{\nu_\mu} , \tag{3}$$

where $g_A = -\frac{1}{2}$, $g_V = \frac{1}{2}(4 \sin^2\theta_W - 1)$ and we take the current[5] value $\sin^2\theta_W = 0.23$.

In the equivalent photon approximation (see, e.g., Ref. 6) the Coulomb field of the target nucleus is replaced by an equivalent on-shell transverse photon flux and the cross section can be written, for a spin-0 target,

$$d\sigma(\mu Z \to \mu \nu \bar{\nu} Z) = \frac{\alpha Z^2}{\pi} \int d\hat{s}\, dQ^2 F_N{}^2(Q^2)(Q^2 - Q_0{}^2) Q^{-4} (1-y)\, d\sigma(\mu\gamma \to \mu\nu\bar{\nu}) . \tag{4}$$

Here α is the fine-structure constant, Z is the nuclear charge, $\hat{s}$ is the invariant mass squared of the final $\mu\nu\bar{\nu}$ system, $-Q^2$ is the invariant squared momentum transfer to the nucleus, $F_N(Q^2)$ is the nuclear form factor, and $Q_0{}^2$ is the kinematical limit of Q^2 given to good approximation by

$$Q_0{}^2 = m_T{}^2 (\hat{s} - m_\mu{}^2)^2 / [(s - m_T{}^2 - m_\mu{}^2)(s - m_T{}^2 - \hat{s})] , \tag{5}$$

where m_T is the target mass and s is the overall invariant mass squared. Also, y is defined by

$$y = (\hat{s} - m_\mu{}^2)/(s - m_T{}^2 - m_\mu{}^2) . \tag{6}$$

For a spin-$\frac{1}{2}$ target the factors $(Q^2 - Q_0{}^2)(1-y)$ of Eq. (4) are replaced by $[Q^2(1 - y + \frac{1}{2}y^2) - Q_0{}^2(1-y)]$. For proton targets we take the usual dipole electric form factor,[7]

$$F_N(Q^2) = [1 - Q^2/(0.71\ \text{GeV}^2)]^{-2} . \tag{7}$$

For complex nuclear targets with atomic number A we take[8]

$$F_N(Q^2) = \frac{B}{Q \sinh(\pi a Q)} [\pi a \sin(cQ) \coth(\pi a Q) - c \cos(cQ)] ,$$
$$B = 3\pi a c^{-1} (c^2 + \pi^2 a^2)^{-1} , \quad a = 0.57\ \text{fm} , \quad c = (1.18 A^{1/3} - 0.48)\ \text{fm} . \tag{8}$$

The equivalent photon approximation relies on Q^2 being very small, which is ensured by the nuclear form

factor and may be confirmed in the calculation. In this limit the equivalent photon flux is essentially collinear with the incident beam in the laboratory so that the azimuthal dependence of the $\gamma\mu\to(\nu\bar{\nu})\mu$ scattering is effectively averaged.

The cross section for the subprocess $\mu\gamma\to\mu\nu_i\bar{\nu}_i$ for given neutrino flavor i can be calculated by standard trace techniques and finally reduced to the following simple form:

$$\frac{d\sigma(\mu\gamma\to\mu\nu_i\bar{\nu}_i)}{dM\,d\hat{t}}=\frac{\alpha G_F^2 M^3}{12\pi^2(\hat{s}-m^2)^2}\times\sum_{k=A,V}g_k^2(i)\left\{\left[\frac{\hat{u}-m^2}{m^2-\hat{s}}+\frac{\hat{s}-m^2}{m^2-\hat{u}}\right](1+2\delta_{kA}m^2/M^2)-4\delta_{kA}m^2/M^2 +2(M^2+2m^2\delta_{kV}-4m^2\delta_{kA})\left[\left[\frac{m}{\hat{s}-m^2}+\frac{m}{\hat{u}-m^2}\right]^2-\frac{\hat{t}}{(\hat{s}-m^2)(\hat{u}-m^2)}\right]\right\}. \tag{9}$$

Here M is the $\nu\bar{\nu}$ invariant mass, m is the muon mass, $\hat{s}$ is the total c.m. energy squared as before, $\hat{t}$ is the invariant square of momentum transfer to the muon and $\hat{u}=2m^2+M^2-\hat{s}-\hat{t}$ is the third Mandelstam variable. The effective weak couplings $g_k(i)$ are defined by

$$g_A(i)=-\tfrac{1}{2}+\delta_{i\mu}\,, \tag{10}$$

$$g_V(i)=2\sin^2\theta_W-\tfrac{1}{2}+\delta_{i\mu}\,. \tag{11}$$

The $\delta_{i\mu}$ terms are due to the W-exchange process [Fig. 1(b)].

The cross section of Eq. (9) has been integrated over azimuthal angle and refers to unpolarized incident muons. For μ^- beams with helicity ±1 (or μ^+ beams with helicity ∓1) the dominant terms in this cross section are modified by factors $F^\pm$ given by

$$F^\pm=(g_V\mp g_A)^2/(g_V^2+g_A^2)\,. \tag{12}$$

These factors give the polarization corrections to order $m^2/\hat{s}$, m^2/M^2, which is a good approximation on the whole since $\hat{s}$ and M^2 turn out to have mean values much greater than m^2. Hence for a typical high-energy μ^+ beam with 70% polarization (i.e., 85% helicity -1, 15% helicity $+1$) the production of $\nu_i\bar{\nu}_i$ pairs is about 43% (89%) of the unpolarized cross section for $i=\mu$ ($i\neq\mu$). With this polarization the W-exchange diagram contributions are suppressed.

Equations (4)–(12) completely define the differential cross section $d\sigma(\mu Z\to\mu\nu_i\bar{\nu}_i Z)/dM\,dQ^2\,d\hat{s}\,d\hat{t}$ and hence the dependence on all kinematical variables except the internal orientation of the $\nu_i\bar{\nu}_i$ pair (which is unmeasurable and has been integrated) and azimuth (that has been integrated). The interesting observables in practice are the energy E' and angle θ of the final muon in the laboratory frame. By evaluating variables in the incident muon rest frame and making a Lorentz transformation, we found the following simple expressions in the collinear approximation:

$$E'=E(m^2-\hat{u})/(\hat{s}-m^2)+O(E^{-1})\,, \tag{13}$$

$$\theta^2=E^{-2}m^2(\hat{s}-m^2+M^2)/(m^2-\hat{u})+O(E^{-4})\,, \tag{14}$$

where E is the incident muon energy. Hence at given $\hat{s}$

$$M^2\simeq(\hat{s}-m^2)(\theta^2EE'/m^2-1)\,, \tag{15}$$

$$-\hat{t}\simeq(\hat{s}-m^2)(2-E'/E-\theta^2EE'/m^2) \tag{16}$$

and we can reexpress the cross section in terms of laboratory variables using

$$\frac{d\sigma}{M\,dM\,d\hat{t}}\simeq\frac{m^2}{E'(\hat{s}-m^2)^2}\frac{d\sigma}{d\cos\theta\,dE'}\,. \tag{17}$$

This approximation fails at very small E', however. For the numerical results reported below, we made Monte Carlo integrations with exact kinematics.

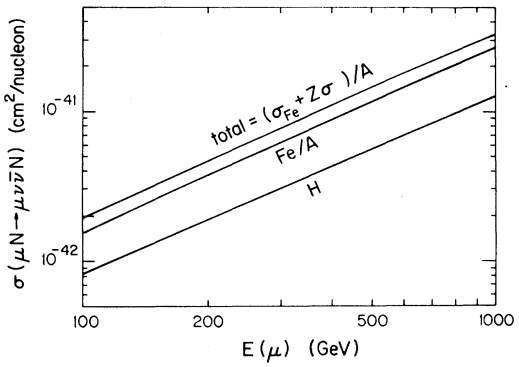

FIG. 2. Total cross sections per nucleon for producing three generations of neutrino pairs versus incident muon energy E. Coherent Coulomb cross sections for Fe and H targets are shown; the combined effect of coherent nuclear plus incoherent single-proton contributions is also shown for an Fe target.

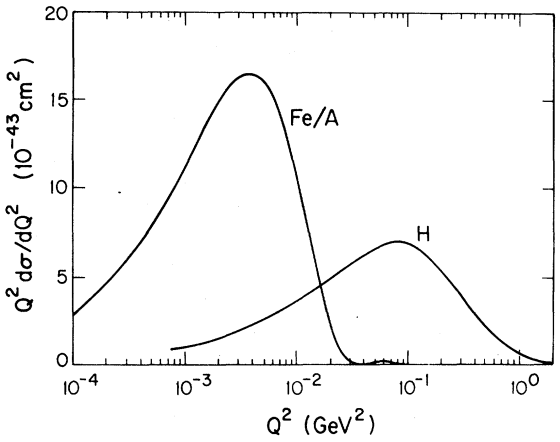

FIG. 3. Q^2 dependence of neutrino pair production (three generations) at muon laboratory energy $E=280$ GeV, for coherent Fe and H targets.

Similar formulas apply to $\nu\bar{\nu}$ production by electron beams, with $m=m_e$.

III. CROSS-SECTION RESULTS

Figure 2 shows the calculated total cross sections *per nucleon* for coherent production on Fe and H targets, summed over three neutrino flavors ν_i ($i=e,\mu,\tau$), versus incident muon energy. The numerical values are very small at accessible energies. For comparison, we note that major contemporary muon experiments in the 200–300 GeV range have integrated luminosities of order 10^{39} cm^2 or less; such experiments are unlikely to produce neutrino pairs at all unless there are many hundreds of neutrino flavors.

With Fe targets we expect incoherent contributions from individual protons recoiling elastically, in addition to the coherent contribution in which the nucleus recoils as a whole. The net effect is to give approximately $[\sigma(\mathrm{Fe})+Z\sigma(\mathrm{H})]/A$ as the cross section per nucleon; this is shown also in Fig. 2. This approximation ignores small contributions from individual neutrons and from hadron production at the nuclear vertex; these are calculated to be very small in the closely analogous case of muon trident production.[9] We also ignore various semicoherent effects in which a subset of nucleons recoils collectively; these are hard to estimate but are commonly neglected. Finally, we have neglected two-photon exchange, which presumably gives corrections of order $\alpha Z \simeq 20\%$ for Fe. Because of these theoretical uncertainties and also the very small cross section, neutrino pair production is not suited to an exact determination of the number of neutrino flavors, but it may be used to set an upper limit and may eventually give an approximate determination of this number.

The calculated cross section increases as s ln$s$. It is also approximately a factor of 3 higher for ep collisions than for μp collisions at 280 GeV. At a hypothetical ep colliding-beam machine with $\sqrt{s}=200$ GeV, the Coulomb cross section for producing three flavors of $\nu_i\bar{\nu}_i$ is 7.5×10^{-40} cm^2. At such colliders the cross sections are bigger and the theoretical uncertainties are fewer, but these events no longer provide a simple practical signature for their identification, because the solid angle near the beam axis is blind.

At a typical energy $E=280$ GeV we calculate

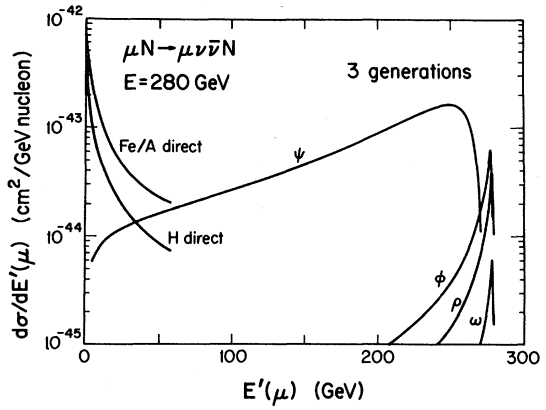

FIG. 4. Final-muon-energy (E') dependence of neutrino pair production (three generations) at $E=280$ GeV, for coherent Fe and H targets. Vector-meson contributions for a single-nucleon target are also shown.

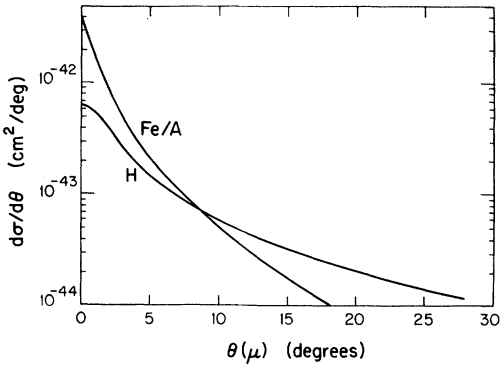

FIG. 5. θ dependence of neutrino pair production (three generations) at $E=280$ GeV, for coherent Fe and H targets.

the following mean values for muoproduction:

	Fe target	H target
$\langle Q^2\rangle$ (GeV^2)	0.005	0.15
$\langle Q_t^2\rangle$ (GeV^2)	0.003	0.11
$\langle E'\rangle$ (GeV)	30.3	23.3
$\langle(\hat{s})^{1/2}\rangle$ (GeV)	3.3	6.5
$\langle M\rangle$ (GeV)	2.4	4.9
$\langle\theta\rangle$ (deg)	2.5	7.3

where $Q_t^2\simeq Q^2-Q_0^2$ is the component of Q^2 transverse to the incident beam axis. These we now discuss.

The very small mean values of Q^2 and Q_t^2 justify the equivalent photon and collinear approximations. The actual shape of the Q^2 distribution is shown in Fig. 3.

The small mean value of E' is at first sight surprising to eyes that are accustomed to electromagnetic or gluonic pair production, where there is a massless propagator factor M^{-2} in the matrix element. In the present case there is no such effect, and phase-space factors encourage M to take up most of the available energy $(\hat{s})^{1/2}$, as can be seen from the numbers above; this leaves the final muon relatively slow in the $\mu\nu\bar{\nu}$ center-of-mass frame and hence in the laboratory too. There is also a $\hat{u}$-channel pole in the cross section Eq. (9), favoring slower μ production through Eq. (13), but numerically the M dependence is the dominant effect. For Fe targets the stronger form factor constrains Q^2 and hence $\hat{s}$ to smaller values; the effect is to make the final muon faster.

TABLE I. $V^0\nu\bar{\nu}$ widths and branching fractions per neutrino flavor.

V^0	$\Gamma(V^0\to\nu\bar{\nu})/\Gamma(V^0\to e^+e^-)$	$\Gamma(V^0\to\nu\bar{\nu})/\Gamma(V^0\to\text{all})$
ρ	$G_F^2 m_\rho^4(x_W-\frac{1}{2})^2/(2\pi\alpha)^2$	7.4×10^{-14}
ω	$G_F^2 m_\omega^4 x_W^2/(2\pi\alpha)^2$	9.8×10^{-14}
ϕ	$G_F^2 m_\phi^4(x_W-\frac{3}{4})^2/(2\pi\alpha)^2$	5.9×10^{-12}
ψ	$G_F^2 m_\psi^4(x_W-\frac{3}{8})^2/(2\pi\alpha)^2$	8.8×10^{-9}
Υ_b	$G_F^2 m_{\Upsilon_b}^4(x_W-\frac{3}{4})^2/(2\pi\alpha)^2$	4.6×10^{-6}
Υ_t	$G_F^2 m_{\Upsilon_t}^4(x_W-\frac{3}{8})^2/(2\pi\alpha)^2$	

Figure 4 shows the actual E' dependence at $E=280$ GeV. The strong peaking at low energy has disadvantages; if we wish the muon to have at least 4 GeV, as commonly required to aid identification, about 28% of the signal is lost with an Fe target (42% with an H target). On the other hand, this peaking helps to distinguish the signal from background (see below).

The scattered muon emerges at appreciable angles, as shown by the mean angle above and by Fig. 5.

IV. CONTRIBUTIONS FROM VECTOR-MESON PRODUCTION

The diffractive production of neutral vector mesons $\mu Z\to\mu V^0 Z$, with $V^0\to\nu\bar{\nu}$ decay, gives a background with a superficially similar missing-energy signature. The branching fractions for $\nu\bar{\nu}$ decay can be calculated by comparing the neutral-current and electromagnetic couplings of the constituent quarks, from which we obtain[10] the formulas and numerical values shown in Table I (with $x_W=\sin^2\theta_W=0.23$), normalizing to the known $V^0\to e^+e^-$ decays. These values should be multiplied by the number of neutrino flavors.

We estimate ρ,ω, and ϕ production on a single nucleon using the following formula, based on vector dominance with purely transverse cross sections:

$$\frac{d\sigma(\mu N\to\mu VN)}{dx\,dy\,dt}=\frac{3m_N m_V{}^3E\Gamma(V\to e^+e^-)}{16\pi^2Q^4(Q^2+m_V{}^2)^2}[\sigma_t(VN)]^2e^{B_V t}[Q^2(2-2y+y^2)-2Q_0{}^2(1-y)]\,, \tag{18}$$

where $\nu=E-E'$, $x=Q^2/(2m_N\nu)$, $y=\nu/E$, t is the invariant momentum-transfer squared in the subprocess

$\gamma N \to VN$, and $Q_0^2 = \nu^2 m_\mu^2 / (EE')$. For the total cross sections we take[11] $\sigma_t(\rho N) = 23$ mb, $\sigma_t(\omega N) = 24$ mb, $\sigma_t(\phi N) = 9$ mb, and for the slope parameters B_V we use[11] $B_\rho = 6.5$ GeV^{-2}, $B_\omega = 6.6$ GeV^{-2}, and $B_\phi = 4.6$ GeV^{-2}.

We estimate diffractive ψ production using the photon-gluon fusion model[12] with parameters chosen to give good agreement[13] with data. We ignore ψ' production that appears to be considerably smaller.[14]

At typical laboratory energy $E = 280$ GeV we calculate the following values for cross section times branching fraction, on a single-nucleon target:

$$\sigma(\mu N \to \mu VN) B(V \to \nu\bar{\nu}) = \begin{cases} 8.6 N_\nu \times 10^{-44} \text{ cm}^2 & (V = \rho^0) \\ 1.4 N_\nu \times 10^{-44} \text{ cm}^2 & (V = \omega) \\ 2.0 N_\nu \times 10^{-43} \text{ cm}^2 & (V = \phi) \\ 5.1 N_\nu \times 10^{-42} \text{ cm}^2 & (V = \psi) \end{cases} \tag{19}$$

summing over N_ν neutrino flavors. Comparison with Fig. 2 shows that the background from ρ, ω, and ϕ production does not compete, but the contribution from ψ production is a factor of 3 greater than the direct neutrino-pair-production signal.

Fortunately, the dependence of the ψ contribution on the final muon energy E' is quite different from that of the direct process. Figure 4 compares the E' dependence of the various contributions for a proton target at $E = 280$ GeV. There is no danger of confusing the ψ and direct $\nu\bar{\nu}$ contribution. Since the ψ contribution can be cleanly separated, and it too depends on N_ν, it can be regarded as an alternative and independent measure of the number of neutrino flavors.

The calculations above for vector-meson production cross sections are simply illustrative. In an eventual neutrino-counting experiment it would be best to normalize to the measured $\mu N \to \mu\psi N$ cross section, based on the $\psi \to \mu^+\mu^-$ decay mode, to avoid theoretical cross-section uncertainties. This is particularly true for complex nuclear targets, where coherent effects are expected.

ACKNOWLEDGMENTS

We thank E. Gabathuler for drawing our attention to this question and for discussions. This research was supported in part by the University of Wisconsin Research Committee with funds granted by the Wisconsin Alumni Research Foundation, and in part by the Department of Energy under Contract No. DE-AC02 76ER00881.

[1] K. Fujikawa, Ann. Phys. (N. Y.) 68, 102 (1971) and references therein.

[2] Wu-Ki Tung, Z. Phys. C 4, 307 (1980). In this paper the relative sign of the Z and W exchange terms in the effective vector coupling is incorrectly given, but the numerical results are not greatly different for $\sin^2\theta_W = 0.23$.

[3] E. Gabathuler, private communication.

[4] The overall signs of H^W and g_A differ from those printed in Ref. 2, but agree with E. S. Abers and B. W. Lee, Phys. Rep. 9C, 1 (1973).

[5] I. Liede and M. Roos, Nucl. Phys. B167, 397 (1980); J. E. Kim, P. Langacker, M. Levine, and H. H. Williams, Rev. Mod. Phys. 53, 211 (1981).

[6] I. Ya. Pomeranchuk and I. M. Shmushkevich, Nucl. Phys. 23, 452 (1961); V. M. Budnev, I. F. Ginzburg, G. V. Meledin, and V. G. Serbo, Phys. Rep. 15C, 181 (1975).

[7] W. Bartel *et al.*, Nucl. Phys. B58, 429 (1973).

[8] I. Zh. Pekov *et al.*, Yad. Fiz. 4, 57 (1966) [Sov. J. Nucl. Phys. 4, 41 (1967)]; M. A. Preston and R. K. Bhaduri, *Structure of the Nucleus* (Addison-Wesley, Reading, Mass., 1975).

[9] V. Barger, W. Y. Keung, and R. J. N. Phillips, Phys. Rev. D 20, 630 (1979); W. Y. Keung, University of Wisconsin—Madison Ph. D. thesis, 1980 (unpublished).

[10] V. Barger and D. V. Nanopoulos, Nucl. Phys. B124, 426 (1977).

[11] V. Barger and R. J. N. Phillips, Nucl. Phys. B97, 452 (1975).

[12] M. A. Shifman, A. I. Vainshtein, and V. I. Zakharov, Nucl. Phys. B136, 157 (1978); J. P. Leveille and T. Weiler, *ibid.* B147, 147 (1979).

[13] V. Barger, W. Y. Keung, and R. J. N. Phillips, Phys. Lett. 91B, 253 (1980).

[14] J. J. Aubert *et al.*, Report No. CERN-EP/80-84 (unpublished).